Enforcing convergence of derivatives for L∞ approximation of a regular curve

Emilien Garcia, J Liandrat

Enforcing convergence of derivatives for L^∞ approximation of a regular curve

E. Garcia[a,b], J. Liandrat[a] *

September 20, 2021

Abstract

Converging approximation of a regular curve by polygonal lines in the uniform norm does not imply the convergence of the discrete differentials to their smooth counterpart. In this paper, we provide a constructive approach that, given a converging polygon sequence and an approximation of its distance to the objective curve, provides another sequence of polygons for which convergence of discrete differentials occurs as well. This approach is based on the notion of local scale of a polygon and uses multi-resolution decomposition as well as a non linear smoothing process. We provide the proof of the convergence and some numerical evidence of it, with application to the evaluation of solid friction in a pipe.

Keywords: Multi-resolution; Subdivision; Smoothing; Derivatives approximation;

Introduction

It is well known that the convergence of a polygon sequence towards a smooth curve in the uniform norm does not imply the convergence of the divided differences of the polygon (i.e. the numerical estimate of its derivatives using finite differences) towards the derivatives of the limit curve. However, in many situations, the simultaneous convergence of a polygon and its derivatives are required. For instance, in the drilling monitoring context, this simultaneous convergence is expected for the wellbore trajectory estimate, which is reconstructed from discrete values, and the friction estimate along the wellbore, that relies on the trajectory derivatives. In the wellbore monitoring framework, there are several methods to provide an approximation of the wellbore trajectory, and there is a general agreement to assert that these methods lead to satisfactory approximations of the real wellbore trajectory. However, the estimates of the derivatives of these approximated trajectories can be very different. This leads to a real difficulty in estimating the friction of the wellbore along the drillstring (directly connected to derivatives up to order 4), while this quantity is essential for the surface monitoring of a wellbore.

This situation has been the main motivation of our work. Reformulating the problem in a mathematical framework, given a sequence of polygons converging towards a smooth function in the uniform norm, is it possible to construct a new sequence of polygons such that these polygons and their derivatives (i.e. their divided differences) of given order simultaneously converge towards the same smooth function and its derivatives of the same order? This question is also relevant in many fields of research and applications such as computer graphics, discrete differential geometry or signal analysis ([1], [2]).

In this paper, it is shown that if the distance between the smooth function and the polygons is controlled, then a construction involving a nonlinear smoothing can be performed. This smoothing relies on a multiresolution decomposition and consists in removing details in a specific procedure illustrated in Figure 1 and described below. In this figure, the black line stands for the unknown smooth curve and the dotted blue lines show the ϵ-tube centred around the curve in which the polygon lies. Observe that the uncontrolled estimate of the first derivative from the piecewise constant slopes of the red polygon is due to the fact that the thickness ϵ of the tube is close to the length of the sides of the polygon. For the "smoothed" polygon (right hand side plot), the length of the segments are increased as much as possible while keeping the polygon inside the tube. The resulting estimates of the derivatives are better. How can we construct automatically this smoothed polygon?

We consider here that the initial polygon is the representation of a sequence belonging to a multiresolution (see section 1.1). In this framework, choosing the linear interpolation of degree 1 as

*[a]Aix-Marseille Univ., CNRS, I2M, UMR7373, Centrale Marseille, 13451 Marseille; [b]Excellence Logging

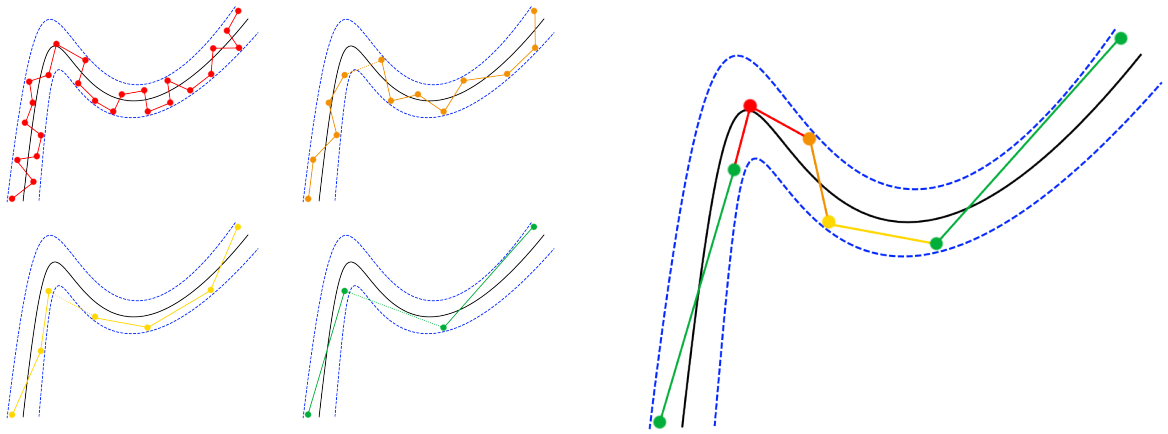

Figure 1: In black, smooth function. In dotted blue, ϵ-tube (top). Left: from left to right then top to bottom, representation of a polygon at different levels of approximation, from higher level (red) to lower level (green); in a sense, polygons green yellow and orange can also be seen as $\epsilon-$independent linear smoothings of the red polygon. Right: non-linearly smoothed polygon.

subdivision, then every other point can be replaced by the midpoint of the two surrounding points plus a small vector from that midpoint to the original point. A first approach could be a linear filtering consisting in cancelling the small vectors associated to every midpoint of the red polygon, as illustrated in Figure 1-left and providing the orange polygon (in the multiresolution terminology the small vectors are called details). Iterating, one also gets the yellow and green polygons. However, this approach does not ensure that the filtered polygons remain at a controlled distance from the black curve. A non-linear smoothing then consists in cancelling locally the details *as long as* the corresponding smoothed polygon remains inside the ϵ-tube, otherwise in keeping them. Iterating, one gets the final polygon illustrated in Figure 1-right. From Figure 2, the discrete derivatives (slope of each line segment) of this polygon are closer to the derivatives of the smooth function than the ones of the original polygon.

Our algorithm is a refined version of this non-linear filtering and aims to build a polygon in an $\epsilon-$tube with a minimal local scale (see next section) at every point. The building elements of our construction are the multiresolution analysis in the framework of A. Harten ([3]) and finite difference operators for approximation of derivative operators in their basic form available in classical textbooks ([4]).

In Preliminaries (Section 1), stable multiresolution analyses of order p and regularity m and their properties are presented with emphasis on the decay of detail coefficients versus scale for a regular function. Among others, the notion of $p, \epsilon-$local level associated to a polygon is presented. Standard properties of finite difference operators as well as some results on the coupling with multiresolution are also recalled. Sections 2 and 3 are devoted to the main contribution of this paper; in Section 2, starting from a polygon sequence converging towards a smooth function, the construction of a new sequence converging, as well as its discrete derivatives (finite differences) up to a given order, to the function and its corresponding derivatives is proposed. Its mathematical analysis is provided in Section 3. Numerical evidences and application to a trajectory in wellbore monitoring are presented in Section 4 while some generalizations and concluding remarks are provided in the last section.

1 Preliminaries

In the sequel of this paper, the integer j (or *scale parameter*) is related to the length 2^{-j}, while the integer k is related to the position $x_k^j = k2^{-j}$ for any j. For a given $j \in \mathbb{Z}$, the sequence $X^j = \left(X_k^j\right)_{k\in\mathbb{Z}}$ also denotes the planar polygon with vertices $\left(k2^{-j}, X_k^j\right)_{k\in\mathbb{Z}}$. For a given continuous function f and a given integer J, the sequence $f^J = \left(f(k2^{-J})\right)_{k\in\mathbb{Z}}$ is called the sampling polygon of f at scale J. It is a piecewise linear interpolation of f.

1.1 Multiresolution Analysis

In this paper, following [5], we consider a fully discrete definition of multiresolution analysis, initially introduced by A. Harten ([3]). It is based on a couple of consistent subdivision ([6]) and

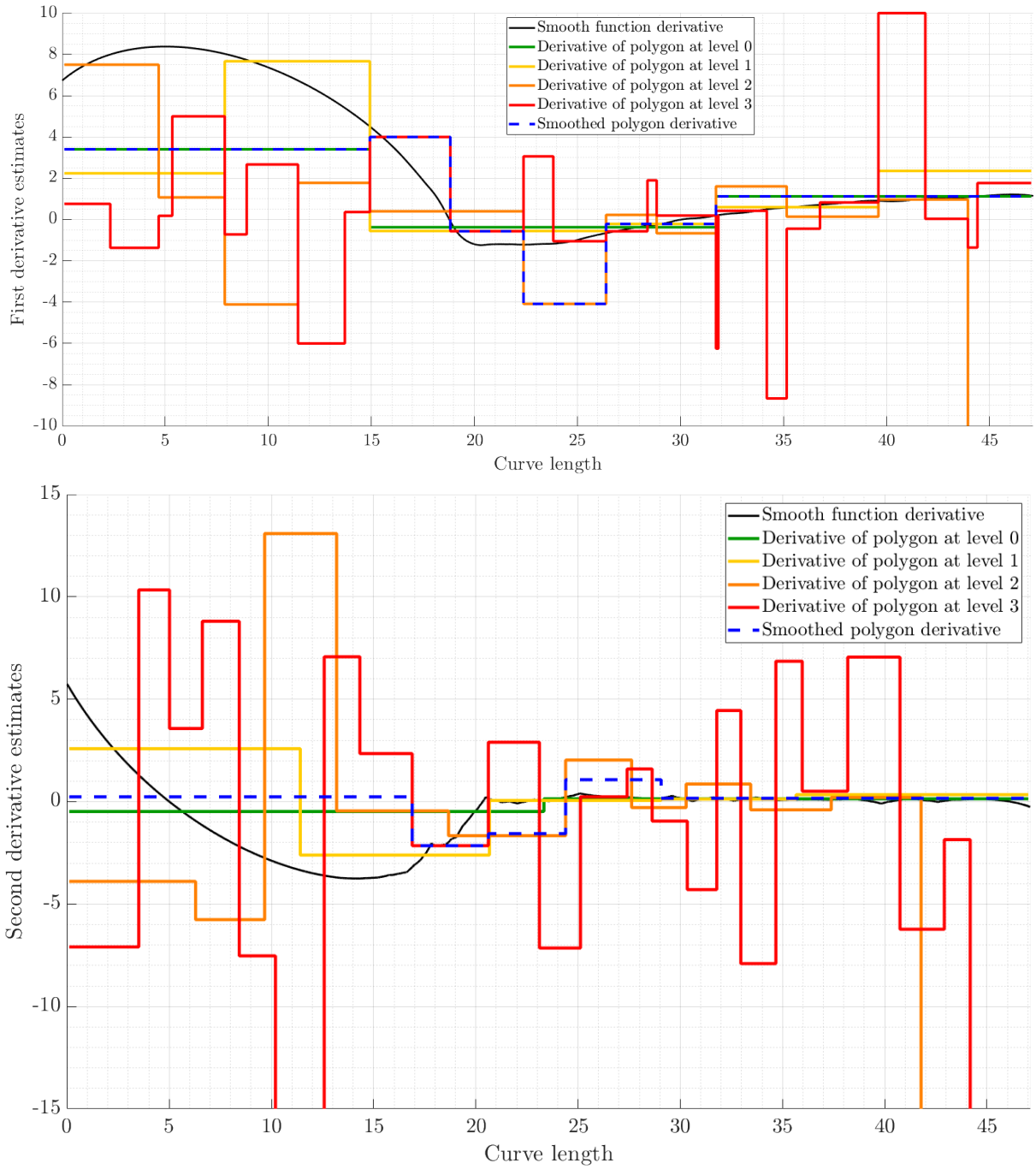

Figure 2: Derivative estimates of the black curve and the polygons introduced in Figure 1. Top (resp. bottom): first order (resp. second order) divided differences associated to each polygon at each approximation level (i.e. each linear smoothing of the red polygon) and to the non-linearly smoothed polygon compared to the first (resp. second) derivative of the regular curve.

decimation operators. Here we consider dyadic linear operators, therefore we have:

Definition 1 (Subdivision/Decimation/Detail)**.** *A* subdivision *operator $S : l^\infty(\mathbb{Z}) \to l^\infty(\mathbb{Z})$ is a linear operator defined through a sequence $(a_k)_{k\in\mathbb{Z}}$ having a finite number of non-zero coefficients such that: For all $X = (X_k)_{k\in\mathbb{Z}}$, SX is defined as $\forall k \in \mathbb{Z}, (SX)_k = \sum_{l\in\mathbb{Z}} a_{k-2l}X_l$. Here, we only consider* converging *subdivision operators, i.e. such that for any initial sequence X, the iterated sequences S^jX converge (uniformly on any compact set) towards a continuous function denoted $S^\infty X$ and called the* limit function *associated to X.*

A decimation *operator $D : l^\infty(\mathbb{Z}) \to l^\infty(\mathbb{Z})$ is a linear operator defined through a sequence $(b_k)_{k\in\mathbb{Z}}$ having a finite number of non-zero coefficients such that: $\forall X = (X_k)_{k\in\mathbb{Z}}$, DX is defined as $\forall k \in \mathbb{Z}, (DX)_k = \sum_{l\in\mathbb{Z}} b_{l-2k}X_l$.*

Two operators S and D are said to be consistent *as soon as $DS = I$, where I stands for the identity operator.*

For two consistent operators S and D, the operator $I - SD$ is called the prediction error *operator. If Π is (up to an isomorphism) a projection on the kernel of D, then $\Pi(I - SD)$ is called the* detail *operator.*

Definition 2 (Basic limit function)**.** *If $\delta_k = \delta_{k,0}$ for all $k \in \mathbb{Z}$, where $\delta_{k,0}$ is the Kronecker symbol, the limit function associated to the sequence $(\delta_k)_{k\in\mathbb{Z}}$, denoted with Φ, is called the* basic limit function *of the subdivision operator S.*

Since the sequence $(a_k)_{k\in\mathbb{Z}}$ has a finite number of non zero coefficients, the basic limit function Φ has a compact support. For $(j, k) \in \mathbb{Z}^2$, $x \in \mathbb{R}$, we denote $\Phi_{j,k}(x) = \Phi(2^jx - k)$.

For any sequence X, denoting $e = (I - SD)X$ and $d = \Pi e$, there exists a bijection between X and the couple (DX, d) (called one scale decomposition) as sketched on Figure 3. Given $J \in \mathbb{Z}$, for any $j_0 < J$ and initial sequence $(X^J_k)_{k\in\mathbb{Z}}$, iterating $X^{j-1} = DX^j, d^{j-1} = \Pi(I - SD)X^{j-l+1}$ provides the sequence $\{X^{j_0}, d^{j_0}, ..., d^{J-1}\}$ called the *multiresolution decomposition* of X^J. The multiresolution reconstruction provides X^J from the sequence $\{X^{j_0}, d^{j_0}, ..., d^{J-1}\}$.

Figure 3: For a given $j \in \mathbb{Z}$, one scale decomposition (left) and reconstruction (right) with $X^j = SX^{j-1} + e^j$ and $d^{j-1} = \Pi e^j$.

The analysis of a multiresolution (essentially the behaviour of the details d^j when j increases) is deeply connected to the behaviour of the differences $\left((\delta X^j)_k = X^j_{k+1} - X^j_k\right)_{k\in\mathbb{Z}}$ along the scales j (see section 1.2). A key property of a multiresolution is its *stability.*

Definition 3 (Stability of the Multiresolution Analysis)**.** *The multiresolution reconstruction is said to be* stable *if there exists $C_r > 0$ such that, for all $j \in \mathbb{Z}$, for all $j_0 < j$, and for all sequences f^j and g^j and their decompositions $\left\{f^{j_0}, d^{j_0}_f, \ldots, d^{j-1}_f\right\}$ and $\left\{g^{j_0}, d^{j_0}_g, \ldots, d^{j-1}_g\right\}$:*

$$\left\|f^j - g^j\right\|_\infty \leq C_r \left(\left\|f^{j_0} - g^{j_0}\right\|_\infty + \sum_{i=j_0}^{j-1} \left\|d^i_f - d^i_g\right\|_\infty\right) \tag{1}$$

The multiresolution decomposition is said to be stable *if there exists $C_d > 0$ such that for all $j_0 < j \in \mathbb{Z}$ and all sequences f^j and g^j and their decompositions $\left\{f^{j_0}, d^{j_0}_f, \ldots, d^{j-1}_f\right\}$ and $\left\{g^{j_0}, d^{j_0}_g, \ldots, d^{j-1}_g\right\}$:*

$$\left\|f^{j_0} - g^{j_0}\right\|_\infty + \sum_{i=j_0}^{j-1} \left\|d^i_f - d^i_g\right\|_\infty \leq C_d \left\|f^j - g^j\right\|_\infty \tag{2}$$

The multiresolution analysis is said to be stable *if both multiresolution reconstruction and decomposition are stable.*

Dealing with consistent couples of linear subdivision and decimation operators, according to [5], the stability is ensured as soon as the subdivision operator is convergent.

In this paper, we will consider subdivision schemes converging towards basic limit functions of regularity $\mathcal{C}^m(\mathbb{R})$. Such subdivision schemes must quasi-reproduce polynomials of degree p with

$p \geq m$, where quasi-reproduction of polynomials of degree p means that the subdivision of the sampling of any polynomial of degree less than or equal to p produces the sampling of a polynomial of the same degree. Generally, we say that the associated multiresolution analysis is of order p and regularity m. Propositions 1 and 2 recall essential properties of multiresolution analysis of order p and regularity m.

One of the advantages of the multiresolution representation of an initial sequence f^J stands in the fact that under the order p hypothesis, the amplitude of the details d_k^j decays when j increases. Indeed, we have the following proposition ([5]):

Proposition 1. *[Decay of the details]*
Given $J \in \mathbb{N}$ and $f \in \mathcal{C}^\infty(\mathbb{R})$, let $f^J := \left(f\left(k2^{-J}\right)\right)_{k\in\mathbb{Z}}$ be the sampling of f. For all $j < J$, let $\left\{f^j, d^j, d^{j+1}, \ldots, d^{J-1}\right\}$ be a decomposition of f^J down to level j using a multiresolution analysis of order p.

Then there exists $C_{dec} > 0$ depending only on f such that for all j:

$$\left\|d^j\right\|_\infty \leq C_{dec} 2^{-j(p+1)} \tag{3}$$

Finally, the localization of the basic limit function Φ (see definition 2) lead to the following definition:

Definition 4 (Local cone)**.** *Let $x_k^j = k2^{-j}$ and S be a linear and convergent subdivision operator with basic limit function Φ. The* local cone *of x_k^j associated to the scheme S is the set $C_S(x_k^j)$ defined by:*

$$C_S(x_k^j) := \left\{(j', k') \text{ such that } x_k^j \in supp\left(\Phi_{j',k'}\right)\right\}$$

where $supp\,(\phi)$ stands for the support of the function ϕ.

1.2 Divided differences and subdivision

All the properties of the multiresolution analysis detailed so far were given in terms of the study of a polygon (or a curve), regardless its related divided differences (or derivatives). In our study, we will consider the following definition and notation for the divided differences of a polygon:

Definition 5 (Divided differences, Stencil)**.** *For $n \in \mathbb{N}$ we denote with Δ_n the* divided differences operator of order n *defined by $\Delta_n = \Delta_1^n$ with $\left(\Delta_1 X^j\right)_k = 2^j(X_{k+1}^j - X_k^j)$ for all $j \in \mathbb{Z}$ and any sequence X^j. It is associated to the sequence of reals $(c_{i,n})_{i\in\mathbb{Z}}$ such that, for all $k \in \mathbb{Z}$:*

$$\left(\Delta_n X^j\right)_k := \frac{1}{(2^{-j})^n} \sum_{i\in\mathbb{Z}} c_{i,n} X^j_{k-\lfloor \frac{n}{2} \rfloor + i} \tag{4}$$

where $\lfloor . \rfloor$ is the floor operator, $c_{i,n} = (-1)^{n-i} \binom{n}{i}$ for all $i \in I_n = \{0, \ldots, n\}$ and $c_{i,n} = 0$ for any other value of i.

We call I_n the stencil *of the operator Δ_n.*

The operator Δ_n is consistent *with the n^{th} derivative up to order q, that means that for any function $f \in \mathcal{C}^\infty(\mathbb{R})$ and its sampling $f_k^j = f(k2^{-j}), k \in \mathbb{Z}$, then:*

$$\left(\Delta_n f^j\right)_k = f^{(n)}\left(k2^{-j}\right) + O\left(2^{-qj}\right) \tag{5}$$

In the multiresolution framework introduced in Section 1.1, a major question arises: when applying a convergent subdivision operator S to an initial sequence f^J, does any convergent subdivision operator exists for the associated order n divided differences $\Delta_n f^j$? In [7] the regularity of the limit function Φ is connected to the existence of a converging scheme for the finite differences.

Indeed, under stability conditions on the basic limit function, the following proposition holds:

Proposition 2. *([6], Theorem 3.4) The subdivision scheme S admits a $\mathcal{C}^m$ limit function if and only if there exists a converging subdivision scheme, S_{Δ_m}, for the divided differences Δ_m.*

Using Definition 1, applying the operator Δ_n and involving S_{Δ_n}, we get, for any sequence X^j:

$$\Delta_n X^j = S_{\Delta_n}\left(\Delta_n X^{j-1}\right) + \Delta_n e^j, \tag{6}$$

with $\left(\Delta_n e^j\right)_k = 2^{nj} \sum_{i\in I_n} c_{i,n} e^j_{k+i}$ for all $k \in \mathbb{Z}$.

This equality shows that the sequences $\left(\left(\left(\Delta_n X^j\right)_k\right)_{k\in\mathbb{Z}}\right)_{J-j_0\leq j\leq J}$ are connected through a multiresolution reconstruction operator associated to the subdivision operator S_{Δ_n} with prediction errors given by $\Delta_n e^j$.

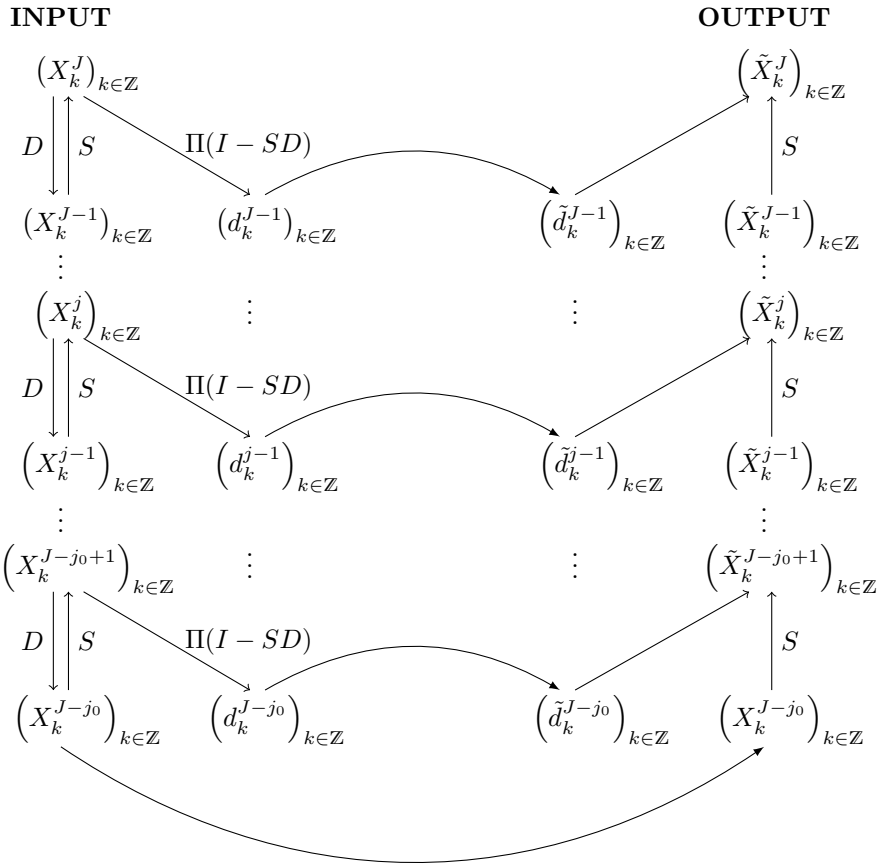

Figure 4: Sketch of a multi-scale smoothing algorithm. The left part is called *multi-resolution decomposition* (step 1), the middle part is called *detail processing* (step 2) and the right part is called *multi-resolution reconstruction* (step 3).

2 Smoothing algorithm improving derivative estimates

A multiresolution smoothing is generally defined using 3 steps. For a given $j_0 < J$:

1. **Multi-resolution decomposition:** starting from level J, decomposition steps are iterated to reach level $J - j_0$;
2. **Detail processing:** details d^j for $J - j_0 \leq j \leq J - 1$ are processed into new details $\tilde{d}^j$;
3. **Multi-resolution reconstruction:** starting from level $J-j_0$, reconstruction steps are iterated to reach level J using the details $\tilde{d}^j, J - j_0 \leq j \leq J - 1$.

These steps are illustrated in Figure 4.

On one hand, the detail processing associated to a low-pass linear filtering of a polygon consists in cancelling all the details above a given level of approximation J_T. Such filtering has been illustrated in Figure 1, where the orange, resp. yellow, resp. green polygon is linearly filtered from the red polygon cancelling all its details above level $J_T = 2$, resp. $J_T = 1$, resp $J_T = 0$. On the other hand, a classical non-linear filtering used in image compression consists in cancelling the details of absolute value smaller than a threshold τ.

In our context, we handle the sampling f^J of a regular function f with step 2^{-J}, and a polygon X^J such that $\left\|X^J - f^J\right\|_\infty < \epsilon$ for a given $\epsilon > 0$. On one hand, a linear filtering cannot smooth the evaluation of the derivatives AND maintain the smoothed polygon into the $\epsilon-$tube (cf. Figure 1); on the other hand, a classical non-linear filtering may not improve the evaluation of the derivatives.

Our goal here is to process the details so that the output smoothed polygon provides better derivative estimates (in a sense that will be precised further), while remaining at distance ϵ of the original curve. The algorithm we propose is detailed in the following section.

2.1 Detail processing

From equation (6) and thanks to stability, $\left\|\Delta_n X^J\right\|_\infty$ is controlled by terms of type $2^{jn}\left|e^j\right|$. The presence of the term 2^{jn} suggests that a way to have a better control on derivative estimates should be to cancel as many details as possible, starting with the details of higher level j, ordering the details by decreasing absolute value. This cancellation has to be performed only if the associated reconstruction remains in the $\epsilon-$tube around X^J, as f^J also lies in this tube.

This detail processing, incorporated as in Figure 4 between a multiresolution decomposition and a multiresolution reconstruction, provides the smoothing algorithm detailed below:

I - Multiresolution decomposition:
X^J is decomposed into the sequences $\left\{X^{J-j_0}, d^{J-j_0}, d^{J-j_0+1}, \ldots, d^{J-1}\right\}$;

II - Details truncation

1) *Initialization:* $\tilde{d}^j := d^j$ for all levels $j \in \{J-j_0, \ldots, J-1\}$;
2) For all levels j from highest $(J-1)$ to lowest $(J-j_0)$:
   - For all $\left|\tilde{d}_k^j\right|$ sorted in decreasing order (then starting from higher values):
     (a) Set $\tilde{d}_k^j := 0$;
     (b) *Multiresolution reconstruction:* $\tilde{X}^J$ is constructed from the decomposition given by $\left\{X^{J-j_0}, \tilde{d}^{J-j_0}, \tilde{d}^{J-j_0+1}, \ldots, \tilde{d}^{J-1}\right\}$;
     * If $\left\|\tilde{X}^J - X^J\right\|_\infty < \epsilon$, then proceed with the next $\tilde{d}_{k'}^{j'}$;
     * If not, set back $\tilde{d}_k^j := d_k^j$, then proceed with the following $\tilde{d}_{k'}^{j'}$;
3) *Stopping condition:*
   (a) If step 2) results in no modification of the sequences $\tilde{d}^j$ for all levels $j \in \{J-j_0, \ldots, J-1\}$, then stop;
   (b) Otherwise, repeat steps 2) and 3);

III - Multiresolution reconstruction:
$\left\{X^{J-j_0}, \tilde{d}^{J-j_0}, \tilde{d}^{J-j_0+1}, \ldots, \tilde{d}^{J-1}\right\}$ are used to reconstruct $\tilde{X}^J$;

2.2 $p, \epsilon-$ smoothing operator and local scale

The previous algorithm depends on the following parameters:

- the real $\epsilon > 0$, controlling the $\epsilon-$tube such that $\left\|X^J - f^J\right\|_\infty < \epsilon$ and $\left\|\tilde{X}^J - X^J\right\|_\infty < \epsilon$;
- the order p of the multiresolution analysis, controlling the decay of the detail coefficients;
- the regularity m of the multiresolution analysis, providing the existence of a convergent subdivision scheme for the order m divided differences;
- the highest derivative order n that we want to estimate accurately using $\tilde{X}^J$;
- the accuracy order q for the finite difference operator Δ_n (i.e. 1 if n is odd and 2 otherwise).

If n and q are imposed by the problem to solve, p m and ϵ can be chosen independently. In the sequel of this paper we consider a given subdivision of order p.

Definition 6 (Smoothing operator $L_{p,\epsilon}$)**.** *For any $J \in \mathbb{Z}$ and any $\epsilon > 0$, the operator $L_{p,\epsilon}$ is defined from $l^\infty(\mathbb{Z})$ to $l^\infty(\mathbb{Z})$ as $X^J \mapsto L_{p,\epsilon}(X^J) = \tilde{X}^J$.*

Moreover, using the local cone C_S (Definition 4):

Definition 7 ($p, \epsilon-$local level)**.** *For $\epsilon > 0$, $p \in \mathbb{N}$, $J \in \mathbb{Z}$ and a given multiresolution of order p, for any $X^J \in l^\infty(\mathbb{Z})$, the order p multiresolution analysis of X^J defines, for all $k \in \mathbb{Z}$, the $p, \epsilon-$*local level *denoted $j_{p,\epsilon}\left(X^J, k2^{-J}\right)$ of X^J at position $k2^{-J}$ as follows:*

$$j_{p,\epsilon}\left(X^J, k2^{-J}\right) := \min\left\{j \leq J \text{ such that } \left[\forall j' > j \text{ such that } (j',k') \in C_S\left(k2^{-J}\right), d_{k'}^{j'-1} = 0\right]\right\}$$

2.3 Error control between the divided differences of f^J and its smoothing

This definition of $p, \epsilon-$local level highlights that the value X_K^J depends on all the values X_k^j as long as $(j,k) \in C_{S_p}(x_K^J)$ where S_p is the subdivision operator of the considered smoothing. Furthermore, from the definition of the order n divided differences operator Δ_n, the derivative estimate at a given point x_K^J of a polygon depends on a given number of points defined by the stencil I_n. Combining these two considerations, the derivative estimate at a given point x_K^J depends on all the points x_k^j as long as (j,k) belongs to the local cone of any point involved in the stencil of the associated divided difference.

This observation allows us to define the local level associated to the stencil of divided differences:

Definition 8 ($p, \epsilon-$stencil local level)**.** *Given $\epsilon > 0$, $p \in \mathbb{N}$, $(J,k) \in \mathbb{Z}^2$, $X^J \in l^\infty(\mathbb{Z})$, and the stencil I_n associated to the operator Δ_n, the $p, \epsilon-$*stencil local level *of X^J at position $k2^{-J}$ is defined as:*

$$j_{\Delta_n,p,\epsilon}\left(X^J, k2^{-J}\right) := \min_{i \in I_n} j_{p,\epsilon}\left(X^J, (k+i)2^{-J}\right),$$

where $j_{p,\epsilon}$ refers to Definition 7.

We also need to define the norm we use to assess the performance of the smoothing algorithm:

Definition 9 ($\infty, K-$norm)**.** *Given $J \in \mathbb{Z}$, for any sequence $X^J = \left(X_k^J\right)_{k\in\mathbb{Z}}$ and any compact $K \subseteq \mathbb{R}$, we define $\left\|X^J\right\|_{\infty,K} := \sup_{\substack{k \in \mathbb{Z} \\ k2^{-J} \in K}} \left|X_k^J\right|$ as the usual norm on $l^\infty(\mathbb{Z})$ restricted to positions in K.*

The following Lemma then relates the finite difference values of the initial polygon f^J to those of its smoothing $L_{p,\epsilon}(f)$. Its proof can be found in Appendix A.

Lemma 1. *Let $\epsilon > 0$, $J \in \mathbb{Z}$, $f \in \mathcal{C}^\infty(\mathbb{R})$ and $f^J = \left(f(k2^{-J})\right)_{k\in\mathbb{Z}}$ be its sampling polygon at scale J. Then, on any compact set K, there exists $C_L > 0$ such that:*

$$\left\|\Delta_n f^J - \Delta_n\left(L_{p,\epsilon} f^J\right)\right\|_{\infty,K} \leq C_L \epsilon^{1-\frac{n}{p+1}}$$

3 Joint Convergence of polygon and finite differences

In this section, for $f \in \mathcal{C}^\infty(\mathbb{R})$ and f^J its sampling polygon at scale J, we introduce X^J, a polygon at scale J such that $\left\|f - X^J\right\|_\infty < \epsilon$.

Supposing that neither f nor f^J are known, for a given smoothing process $L_{p,\epsilon}$, we would like to estimate the derivatives of f using the divided differences of $L_{p,\epsilon}X^J$, with a control based upon the related estimation error ϵ.

The main ingredient for this estimate is the construction of a polygon g^J, obtained from $L_{p,\epsilon}X^J$ by discarding some details AND having the same local scale as $L_{p,\epsilon}f^J$.

3.1 Existence of a polygon with the same local levels in an $\epsilon-$tube

The proof of the following proposition can be found in Appendix B.

Proposition 3.

Let $\epsilon > 0$, $f \in \mathcal{C}^\infty(\mathbb{R})$ and $f^J = \left(f(k2^{-J})\right)_{k\in\mathbb{Z}}$ its sampling polygon at scale J. Let also $X^J = \left(X_k^J\right)_{k\in\mathbb{Z}}$ be a polygon such that: $\left\|f^J - X^J\right\|_\infty < \frac{\epsilon/2}{1+C_rC_d}$, where C_r and C_d are the respective stability constants for the multiresolution reconstruction and decomposition.

Then there exists a polygon g^J, constructed from a smoothing of X^J, such that $\left\|X^J - g^J\right\|_\infty < \epsilon$, $\left\|f^J - g^J\right\|_\infty < \epsilon$, and whose local levels are at most the local levels of $L_{p,\frac{\epsilon/2}{1+C_rC_d}} f^J$ for all $k \in \mathbb{Z}$.

3.2 Error control between the divided differences of $L_{p,\epsilon}f^J$ and $L_{p,\epsilon}X^J$

The proof of the following lemma can be found in Appendix C.

Lemma 2.

Let $\epsilon > 0$, $K \subseteq \mathbb{R}$ be a compact, $f \in \mathcal{C}^\infty(\mathbb{R})$ and $f^J = \left(f(k2^{-J})\right)_{k\in\mathbb{Z}}$ be the sampling polygon of f at scale J. Let also $X^J = \left(X_k^J\right)_{k\in\mathbb{Z}}$ be a polygon such that $\left\|f^J - X^J\right\|_\infty < \frac{\epsilon/2}{1+C_rC_d}$.

Then there exists $C > 0$ such that:

$$\left\|\Delta_n\left(L_{p,\epsilon}f^J\right) - \Delta_n\left(L_{p,\epsilon}X^J\right)\right\|_{\infty,K} \leq C\epsilon^{1-\frac{n}{p+1}}$$

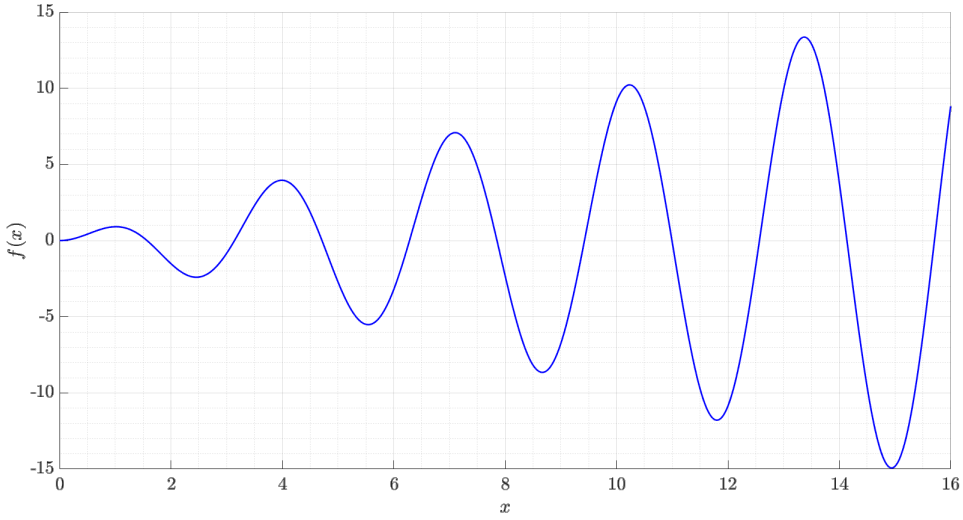

Figure 5: Graph of the function f used for the numerical tests of Section 4.

3.3 Theorem: control of the estimation of $f^{(n)}$ using the divided differences from the smoothing of X^J

Combining Equation (5) with Lemmas 1 and 2, we are now able to prove the following final theorem:

Theorem 1.

Let $\epsilon > 0$, $K \subseteq \mathbb{R}$ be a compact, $f \in \mathcal{C}^\infty(\mathbb{R})$ and $f^J = \left(f(k2^{-J})\right)_{k\in\mathbb{Z}}$ be the polygon describing f at level J. Let also $X^J = \left(X_k^J\right)_{k\in\mathbb{Z}}$ be a polygon such that $\left\|f^J - X^J\right\|_\infty < \epsilon$.

Using a multiresolution analysis of order p and regularity $m(\leq p)$, if there exists a convergent scheme for Δ_n (which requires $m \geq n$), then:

$$\left\|f^{(n)} - \Delta_n\left(L_{p,\epsilon}X^J\right)\right\|_{\infty,K} \leq C_1 2^{-Jq} + C_2\epsilon^{1-\frac{n}{p+1}} \tag{7}$$

Proof.

For sake of simplification, we denote $L := L_{p,\epsilon}$. First, for all $k \in \mathbb{Z}$ such that $k2^{-J} \in K$ we have:

$$\left\|f^{(n)} - \Delta_n\left(LX^J\right)\right\|_{\infty,K} \leq \left\|f^{(n)} - \Delta_n f^J\right\|_{\infty,K} + \left\|\Delta_n f^J - \Delta_n\left(Lf^J\right)\right\|_{\infty,K} + \left\|\Delta_n\left(Lf^J\right) - \Delta_n\left(LX^J\right)\right\|_{\infty,K}$$

Then,

- From Definition 5 and Equation (5), there exists $C_1 > 0$ such that the 1st RHS term is lower than $C_1 2^{-Jq}$;
- From Lemma 1, there exists $C_3 > 0$ such that the 2nd RHS term is lower than $C_3\epsilon^{1-\frac{n}{p+1}}$;
- From Lemma 2, there exists $C_4 > 0$ such that the 3rd RHS term is lower than $C_4\epsilon^{1-\frac{n}{p+1}}$;

Denoting $C_2 := C_3 + C_4$, the expected result is obtained. □

This theorem implies that, to estimate the derivatives of f up to order n with an error controlled by ϵ, the parameter p has to be chosen carefully such that $p \geq n$. In other words, the degree of polynomials quasi-reproduced by S_p must be at least equal to the highest order n of the derivatives of f that we want to estimate with controlled error on ϵ.

4 Validation and Application

In the first part of this section, a manufactured example is analyzed and focuses on numerical evidences of Theorem 1. The second part of this section is devoted to an example of wellbore monitoring where a precise estimate of friction, and therefore derivatives up to 4^{th} order, is compulsory.

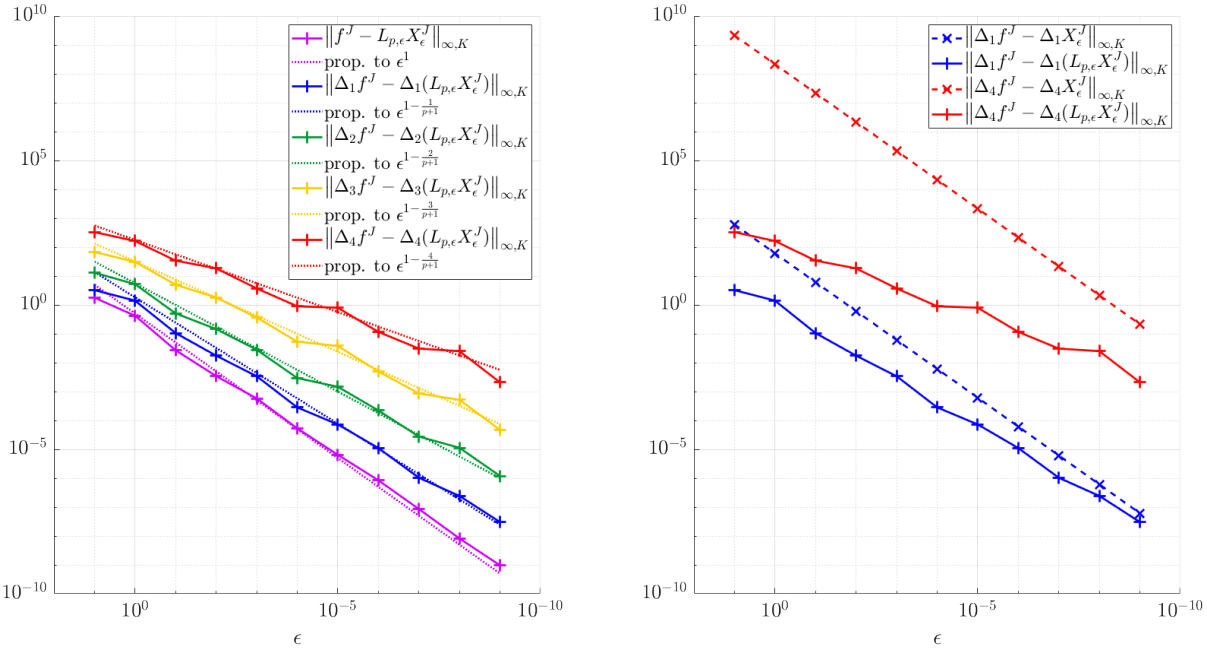

Figure 6: Left: $l^\infty-$norm of the difference between the divided differences of order $1 \leq n \leq 4$ of f^J and those of a smoothing of X_ϵ^J versus ϵ (log-log scale) for a $p = 8, m = 4$ multiresolution (8-point shifted Lagrange). Right: comparison of these estimation errors using X_ϵ^J (dotted line) or its smoothing (continuous line) for the divided differences of order 1 (blue) and 4 (red).

4.1 Numerical tests

The purpose of this section is to show numerical evidences related to Theorem 1. The curve f is defined as the graph of the function $f(x) = x\sin(2x)$ and is plotted in Figure 5. Its sampling $f^J = \left(f_k^J := f(k2^{-J})\right)_{k\in\{0,\dots,1024\}}$ is performed for $J = 6$ on the compact set $[0, 16]$. For $\epsilon > 0$, denoting $\gamma^J = (\gamma_k^J)_{k\in\{0,\dots,1024\}}$ a sequence of random reals uniformly distributed on the segment $[-1, 1]$, we consider the polygon $X_\epsilon^J := f^J + \epsilon\gamma^J$. We will focus on $\left\|\Delta_n f^J - \Delta_n\left(L_{p,\epsilon}X_\epsilon^J\right)\right\|_\infty$ and therefore consider only the second RHS term of equation (7). To avoid edge effects (see implementation details in appendix D.) we will consider in the sequel restrictions to the compact $K = [3, 14]$, where uniformity of the subdivision scheme is verified and mandatory for the validity of Theorem 1.

The smoothing $L_{p,\epsilon}$ of order $p = 8$ and regularity $m = 4$, defined by the 8−point shifted Lagrange subdivision scheme (cf. Appendix D.2 for more details), is used. The parameter J being fixed we plot on Figure 6-left the $l^\infty-$norm of $\left(\Delta_n f^J\right) - \left(\Delta_n\left(L_{p,\epsilon}X_\epsilon^J\right)\right)$ for $1 \leq n \leq 4$ and different values of ϵ.

From Proposition 2, given that $L_{p,\epsilon}$ has regularity $m = 4$, there exists a convergent subdivision schemes for Δ_n for $n \leq 4$. Then, the plotted quantities are expected to decay with a slope $1 - \frac{n}{p+1}$ with $p = 8$.

For each n, the simulation results are represented with crosses of different colors linked with a continuous line, and the expected decay slope $1 - \frac{n}{p+1}$ from Theorem 1 for the error (in logarithmic scale) is represented by a dotted line of the same color.

On this plot, the behaviour of the errors fits with the prediction for values of ϵ higher than 10^{-8} ; below this bound, the error decay fits a slope 1. This behaviour is linked to the fact that the maximum scale parameter $J = 6$ is fixed. Below a certain value of ϵ, for all orders n, the basic error $2^{Jn}\epsilon$ controls the global error since no smoothing is possible and the local level at each position is J.

To exhibit the efficiency of the smoothing, Figure 6-right compares the errors between the divided differences of f^J and the divided differences of $L_{p,\epsilon}X_\epsilon^J$ to the errors between the divided differences of f^J and the divided differences of X_ϵ^J, for the divided differences operators Δ_1 and Δ_4. This plot shows that there are many orders of magnitude of differences between these two errors (up to 6 orders between the divided differences of order 4). In fact, by construction of the polygon X_ϵ^J, the error estimating $\Delta_n f^J$ by using $\Delta_n X_\epsilon^J$ is only controlled by the highest level J, while it is controlled by the local level of X^J using $\Delta_n\left(L_{p,\epsilon}X_\epsilon^J\right)$.

Remark 1. *Our smoothing algorithm stands on many applications of decomposition and reconstruction algorithms that are fast algorithms. The average CPU time involved in the numerical tests of this section is about* 2 *seconds on a Personal Computer equipped with specific libraries for sparse matrix operations.*

Next section focuses on a practical application of the smoothing algorithm to wellbore trajectories by checking that the smoothing process allows to get reliable trajectory derivative estimates, despite the noise in the measurements, permitting to reconstruct the trajectory.

4.2 Application: wellbore trajectories

In the drilling context, wellbore monitoring of efforts at bit can be performed from surface measurements using a friction model. Such a model draws a close relation between surface and bottom efforts according to the soil friction factors. Friction along the wellbore can only be computed if the wellbore trajectory as well as its derivatives up to order 4 are accurately estimated.

For each specific drilling, the optimized wellbore trajectory is planned before drilling the well, which must then be drilled as close to the optimized trajectory as possible. Approximately every $10m$ to $30m$, the direction of the bit at the bottom of the well is measured. These discrete survey measurements then allow to assess the effective wellbore trajectory by reconstruction.

Many reconstruction methods exist to estimate the drillbit location for different drillstring lengths (see [8] for more details). These methods only differ in the shape hypothesis between two survey measurements:

- A circular arc, for the Minimum Curvature Method (MCM, see [9]) which is considered as a reference in the drilling industry;
- A parabolic arc, for the Quadratic Method (QUM, see [10]),
- A helical arc, for the Minimum Torsion Method (MTM, see [10]),
- A polynomial interpolation, like the SIT (see [11]) or the ASC (see [12]),
- etc.

Whatever the chosen reconstruction method, all these estimated trajectories provide bit localization within a $\pm 2m$ uncertainty at the bottom of the well, which is sufficient for drilling purpose (the wellbore length typically reaches $3000m$ to $7000m$, and some wells can still be longer).

However, in the context of friction estimation along the wellbore, derivatives of the reconstructed trajectory also need to be accurately estimated. For example, in the friction model developed in [8], the second order derivative of the curvature of the well must be accurately assessed. Since the curvature itself is a 2^{nd} order derivative of the trajectory, this means that the derivatives of a wellbore trajectory must be accurately estimated up to order 4 for this friction model.

These derivative estimates, though, are highly dependent on the chosen reconstruction method and there is no argument to decide if a method leads to better derivative estimates than another. To show this dependency, on Figure 7-top are drawn the friction charts related to friction endured by the drillstring in the axial (top left) and rotational (top right) directions, using the friction model developed in [8] and the SIT reconstructed trajectory of a well.

On the right, each vertical line stands for the surface rotational friction endured by a rotating drillstring without axial movement (FR for Free Rotating) for a given (but unknown) value of the friction coefficient μ_r constant throughout the well. For a given length of drillstring introduced in the well (vertical axis), the predicted torque endured at surface can be read on the horizontal axis for each value of the coefficient μ_r. The coefficient μ_r increases by 0.01 from a line to its right neighbour up to 0.3 for the last line at the right, the case $\mu_r = 0$ being the vertical axis itself (torque is 0 throughout the well if no friction).

On the left, an equivalent chart is given when the drillstring is either pulled up from the well (PU for Pick-Up) or pushed down into the well (SO for Slack-Off) without rotating. In this case, each line stands for surface drillstring tension predictions for a given value of the friction coefficient μ_a constant throughout the well. With no movement ($\mu_a = 0$), the prediction is given by the blue line. Increasing μ_a with step 0.01 up to value 0.3, two vertical lines are obtained for each value of μ_a: one for PU movement drawn in red (values higher than the blue line and increasing with increasing μ_a), another one for SO movement drawn in yellow (values lower than the blue line and decreasing with increasing μ_a).

Points have been projected on the prediction charts. They stand for synthetic surface measurements of drillstring torque and tension with the expected experimental behaviour through well depth.

The lines of both top charts should become smoother when the length of drillstring introduced in the well increases. More precisely, surface measurements usually follow the trend of a line for given

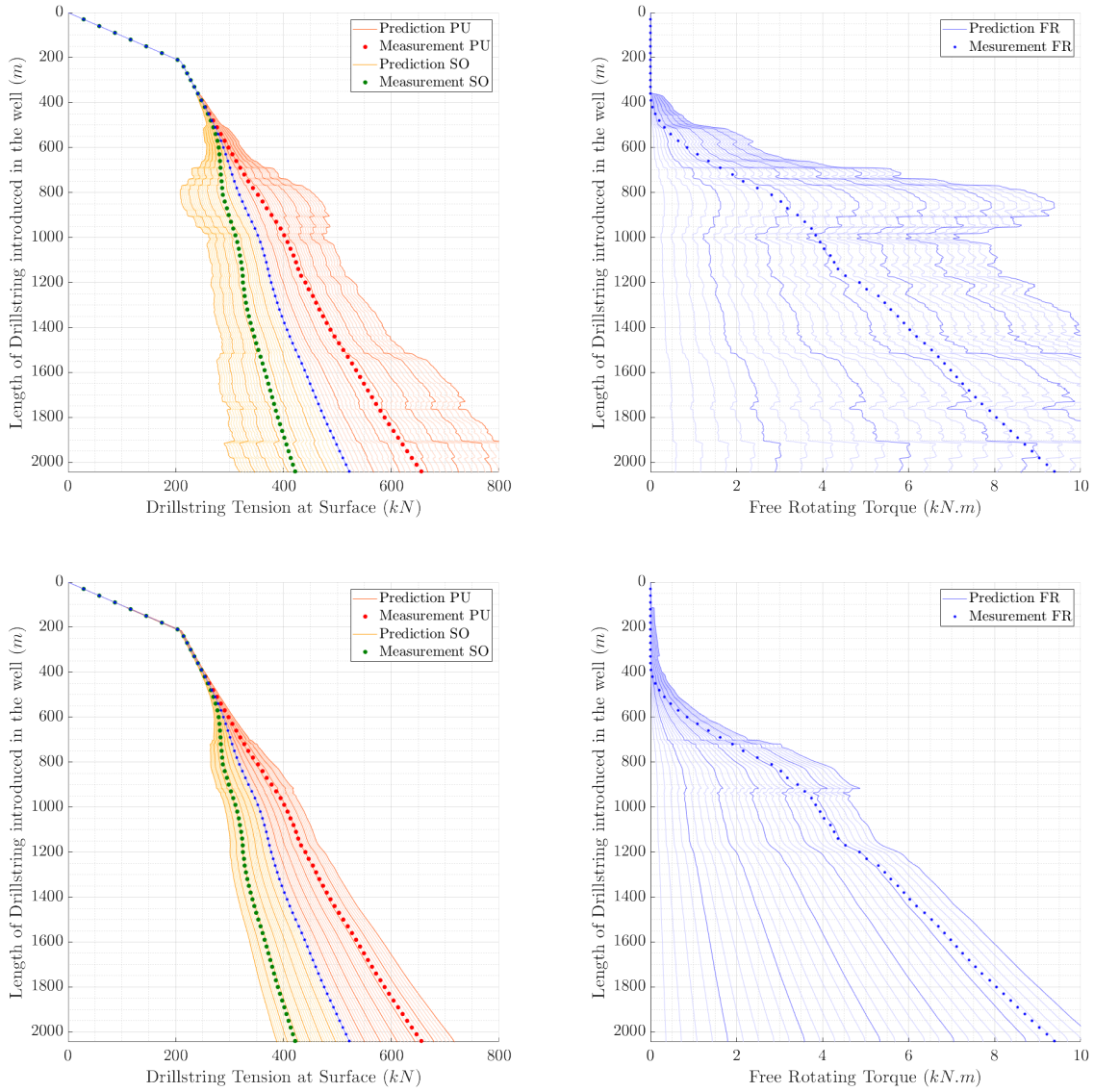

Figure 7: Comparison of the friction charts obtained using the SIT reconstructed trajectory of a well (top) and its smoothing using the 8 points shifted Lagrange scheme (bottom). Left: surface drillstring tension predictions for a drillstring getting in (yellow lines) or out (red lines) the well without rotating (the blue line stands for the case with no axial movement, then with no axial friction). Right: surface frictional torque predictions for a rotating drillstring with no axial movement. For each of them, each vertical line stands for a constant friction factor throughout the well. Projected data over the charts should follow the trend of one vertical line.

μ_a and μ_r values, which means that any variation in the trend of the measurements should also be observed in the predictions. Especially on the torque prediction chart, we can see that data do not manage to follow a constant trend, and that a lot of variations of the prediction lines are not observed in the data trend.

Supposing that the SIT reconstruction method provides a discrete estimation X^J of the real continuous wellbore trajectory f, and that there exists $\epsilon > 0$ such that X^J lies in an $\epsilon-$tube around f, the smoothing process developed in Section 2 can be applied to X^J.

On Figure 7-bottom, the same charts have been realized using the friction model developed in [8] and the smoothing of the SIT reconstructed trajectory performed using the 8-point shifted Lagrange scheme with $\epsilon = 0.1m$. We recall that this scheme generates a smoothing of order $p = 8$ and regularity $m = 4$, while the friction model requires good derivative estimates of the trajectory up to order 4.

In this case, not only the data projected onto the charts better manage to fit a line of constant value for μ_r (around 0.25 after introducing more than $1000m$ of the drillstring), but the constant friction lines of the charts are much smoother than in the upper charts. This implies that poor trajectory derivative estimates lead to poor friction charts to set drillstring/wellbore friction factors, while these factors are essential indicators for drilling safety and prevention.

We should note that three limiting conditions prevented from directly applying the smoothing process of Section 2 to X^J:

1) X^J is a three-coordinate curve defined in space where x y and z are three variables sampled from the drillstring length s, but this sampling has no constant step on s and does not correspond to a natural graph of a function.

Our initial approach, called graph setting, is different from the current one, called curve setting. However, curve setting is a standard extension framework for subdivision: up to a dilation function, both settings coincide.

2) The smoothing algorithm, and more precisely the corresponding subdivision S and decimation D schemes, are defined for an infinite sequence X^J, but here X^J is a finite sequence. As a consequence, S and D must be adapted at both ends of X^J.

At edges, the coefficients involved for S and D must be adapted as described in [13]. For the schemes used in this paper, edges adaptations are precised in Appendix D. However, with this redefinition at edges, the uniformity of the schemes is lost, which is essential for the multiresolution analysis. The efficiency of the smoothing at edges may be lowered.

3) ϵ is not known.

This issue cannot be solved only from a mathematical point of view. Indeed, referring to the comment discussion about Figure 6 in Section 4.1, ϵ must not be chosen too big nor too small for the purpose of getting good estimates of the trajectory and its derivatives. For this application, we decided to give ϵ a physical meaning related to the gap between the drillstrings diameter and the wellbore diameter, that is to say $\epsilon = 0.10m$.

Conclusion

In this paper, a non-linear smoothing has been developed and analyzed. It ensures the simultaneous convergence of a polygon X^J and its divided differences towards a curve f and its derivatives as long as an estimate of the error $\left\|f - X^J\right\|_\infty$ is known.

This smoothing uses a multi-resolution analysis and the notion of $\epsilon-$local scale associated to a smooth curve that characterizes locally its oscillatory behaviour.

Validation of the theoretical properties of the smoothing has been performed using a multiresolution characterized by its high order and regularity. An application of this smoothing for the evaluation of friction efforts along a wellbore trajectory in a drilling context demonstrated the interest of this approach. This application also illustrated some of the various possible adaptation tracks for our approach. Indeed we adapted the construction to non regular sampling as well as to finite length intervals. Further possible developments should deal with noisy scatter graphs using Hausdorff distance. Extension to the approximation of larger dimension unknowns with their specific metric could also be investigated.

Acknowledgement

The authors would like to thank Excellence Logging for sharing drilling data and their friction model in order to validate the developed smoothing algorithm on a practical application.

References

[1] Keenan Crane and Max Wardetzky. A glimpse into discrete differential geometry. *Notices of the American Mathematical Society*, 64(10):1153–1159, 2017.

[2] G Farin, J Hoschek, and M.S Kim. *Handbook of computer aided geometric design*. North Holland, 2002.

[3] Ami Harten. Multiresolution representation of data: A general framework. *SIAM J. Numer. Anal.*, 33(3):1205–1256, 1996.

[4] Robert Dautray and Jacques-Louis Lions. *Analyse mathématique et calcul numérique*. Masson, 1988.

[5] Zhiqing Kui. *On the Construction of Multiresolution Analysis Compatible with General Subdivisions*. PhD thesis, Ecole Centrale de Marseille, France, 2018.

[6] Nira Dyn. Subdivision schemes in computer aided geometric design. In *Light, W.(ed.) Advances in Numerical Analysis II, Wavelets, Subdivision Algorithms and Radial Functions*, pages 36–104. Clarendon Press, Oxford, 1992.

[7] Nira Dyn and Peter Oswald. Univariate subdivision and multi-scale transforms: The nonlinear case. In *Multiscale, Nonlinear and Adaptive Approximation*, pages 203–247. Springer, 2009.

[8] Emilien Garcia. *Approche non-linéaire du monitoring de forage : un espoir de progrès pour la commande en surface ?* PhD thesis, Ecole Centrale de Marseille, France, 2019.

[9] C. J. M. Wolff and J. P. de Wardt. Borehole Position Uncertainty - Analysis of Measuring Methods and Derivation of Systematic Error Model. *Journal of Petroleum Technology*, 33(12):2339–2350, 1981.

[10] J. Kaplan. *Modélisation tridimensionnelle du comportement directionnel du système de forage rotary*. Thèse, ENSMP, 2003.

[11] A. Gfrerrer and G. P. Glaser. A New Approach for Most Realistic Wellpath Computation. *SPE*, 100(3), 2000.

[12] M. F. Abughaban, B. Bialecki, A. W. Eustes, J. P. de Wardt, and S. Mullin. Advanced Trajectory Computational Model Improves Calculated Borehole Positioning, Tortuosity and Rugosity. *SPE/IADC Drilling Conference, Fort Worth, Texas, 1-3 March, SPE-178796-MS*, 2016.

[13] Zhiqing Kui, Jean Baccou, and Jacques Liandrat. *On the Coupling of Decimation Operator with Subdivision Schemes for Multi-scale Analysis*, pages 162–185. Springer International Publishing, Cham, 2017.

A Proof of Lemma 1

Proof. For any fixed value $k \in \mathbb{Z}$ such that $k2^{-J} \in K$, we denote, for simplicity $j_{\Delta_n} := j_{\Delta_n,p,\epsilon}(f^J,k)$, $j_i := j_{p,\epsilon}(f^J,k+i)$ and $L := L_{p,\epsilon}$. We also denote d_f^j (resp. d_{Lf}^j) the details associated to the multiresolution decomposition of f^J (resp. Lf^J) at level j.

By the definition of j_{Δ_n}, for all $i \in I_n$, $f_{k+i}^{j_{\Delta_n}} = \left(Lf^{j_{\Delta_n}}\right)_{k+i}$, and therefore $\Delta_n f_k^{j_{\Delta_n}} = \Delta_n\left(Lf^{j_{\Delta_n}}\right)_k$.

Moreover, due to the decay of the details, for all $i \in I_n$, $2^{-j_i} = O\left(\epsilon^{\frac{1}{p+1}}\right)$ and therefore $2^{-j_{\Delta_n}} = O\left(\epsilon^{\frac{1}{p+1}}\right)$: then there exists $C_\epsilon > 0$ such that $2^{-j_{\Delta_n}} \leq C_\epsilon \epsilon^{\frac{1}{p+1}}$ for all $k \in \mathbb{Z}$ such that $k2^{-J} \in K$.

Finally, using the definition of j_i, for all pairs $(j,l) \in C\left((k+i)2^{-J}\right)$ such that $j > j_i$, we have $d_{Lf,l}^{j-1} = 0$.

As there exists a convergent scheme S_{Δ_n} for the order n divided differences using the order p smoothing, we denote $C_r > 0$ the constant associated to the multiresolution reconstruction stability of the scheme S_{Δ_n}.

Using all these facts successively, for all $k \in \mathbb{Z}$ such that $k2^{-J} \in K$ we have:

$$
\begin{aligned}
\left|\left(\Delta_n f^J\right)_k - \left(\Delta_n(Lf^J)\right)_k\right| &\leq C_r \left[\sup_{(j_{\Delta_n},k_i)\in \bigcup\limits_{i\in I_n} C(x_{k+i})} \left|\left(\Delta_n f^{j_{\Delta_n}}\right)_{k_i} - \left(\Delta_n\left(Lf^{j_{\Delta_n}}\right)\right)_{k_i}\right| \right.\\
&\qquad \left. + \sum_{j=j_{\Delta_n}+1}^{J} \sup_{(j,k_i)\in \bigcup\limits_{i\in I_n} C(x_{k+i})} \left|d_{\Delta_n f,k_i}^{j-1} - d_{\Delta_n Lf,k_i}^{j-1}\right|\right]\\
&\leq C_r \left[\sum_{j=j_{\Delta_n}+1}^{J} 2^{jn} \sum_{i\in I_n} |c_{i,n}| \sup_{(j,k_i)\in C(x_{k+i})} \left|d_{f,k_i}^{j-1} - d_{Lf,k_i}^{j-1}\right|\right]\\
&\leq C_r \sum_{i\in I_n} |c_{i,n}| \sum_{j=j_i+1}^{J} 2^{jn} \sup_{(j,k_i)\in C(x_{k+i})} \left|d_{f,k_i}^{j-1}\right|\\
&\leq C_r \sum_{i\in I_n} |c_{i,n}| \sum_{j=j_i+1}^{J} 2^{jn} C_{dec} 2^{-j(p+1)}\\
&\leq C_r C_{dec} \sum_{i\in I_n} |c_{i,n}| 2^{-j_i(p+1-n)}\\
&\leq 2^{-j_{\Delta_n}(p+1-n)} C_r C_{dec} \sum_{i\in I_n} |c_{i,n}|\\
&\leq \left[C_r C_{dec} \sum_{i\in I_n} |c_{i,n}|\right] C_\epsilon \epsilon^{1-\frac{n}{p+1}} = C_L \epsilon^{1-\frac{n}{p+1}}
\end{aligned}
$$

where $C_L = C_r C_{dec} C_\epsilon \sum\limits_{i\in I_n} |c_{i,n}|$ and C_{dec} is the constant associated to the decay of the details of f^J introduced in Proposition 1.

The expected result is obtained taking the supremum on k. □

B Proof of Proposition 3

Proof.

We simplify the notation and, $\forall k \in \mathbb{Z}$, we denote $j_{f,k} := j_{p,\frac{\epsilon/2}{1+C_rC_d}}(f^J, k2^{-J})$, $j_{g,k} := j_{p,\frac{\epsilon/2}{1+C_rC_d}}(g^J, k2^{-J})$, $C(k) := C_{S_p}(k2^{-J})$ and $L := L_{p,\frac{\epsilon/2}{1+C_rC_d}}$.

Using the definition of the smoothing L and adapting the threshold, we can construct the smoothings of f^J and X^J such that :

$$\left\|f^J - Lf^J\right\|_\infty < \frac{\epsilon/2}{1+C_rC_d}, \qquad \left\|X^J - LX^J\right\|_\infty < \frac{\epsilon/2}{1+C_rC_d}$$

We now define g^J as an over-smoothing of LX^J (i.e. setting details to zero) such that, for all $k \in \mathbb{Z}$ and all $(j,k') \in C(k)$, if $j > j_{f,k}$, then $d^{j-1}_{g_L,k'} = 0$. Thus, for all $k \in \mathbb{Z}$, $j_{g,k} \leq j_{f,k}$. Moreover, for all $k \in \mathbb{Z}$, $g^{j_{f,k}} = LX^{j_{f,k}}$ (no prediction error of X^J has been altered under those levels through this over-smoothing) and $f^{j_{f,k}} = Lf^{j_{f,k}}$ (using the definition of local level).

Using the stability of the multiresolution analysis:

$$\begin{aligned}
\left|\left(Lf^J\right)_k - g^J_k\right| &\leq C_r\left[\sup_{(j_{f,k},k')\in C(k)}\left|\left(Lf^{j_{f,k}}\right)_{k'} - g^{j_{f,k}}_{k'}\right| + \sum_{j=j_{f,k}+1}^{J}\sup_{(j,k')\in C(k)}\left|d^{j-1}_{Lf,k'} - d^{j-1}_{g,k'}\right|\right] \\
&\leq C_r\left[\sup_{(j_{f,k},k')\in C(k)}\left|f^{j_{f,k}}_{k'} - \left(LX^{j_{f,k}}\right)_{k'}\right|\right] \\
&\leq C_rC_d\left|f^J_k - \left(LX^J\right)_k\right| \leq C_rC_d\left\|f^J - X^J + X^J - LX^J\right\|_\infty < C_rC_d\frac{2\epsilon/2}{1+C_rC_d} \\
\implies \left\|Lf^J - g^J\right\|_\infty &\leq C_rC_d\frac{\epsilon}{1+C_rC_d}
\end{aligned}$$

Then:

$$\begin{aligned}
\left\|f^J - g^J\right\|_\infty &\leq \left\|f^J - Lf^J\right\|_\infty + \left\|Lf^J - g^J\right\|_\infty < (\frac{1}{2} + C_rC_d)\frac{\epsilon}{1+C_rC_d} < \epsilon \\
\left\|X^J - g^J\right\|_\infty &\leq \left\|X^J - f^J\right\|_\infty + \left\|f^J - g^J\right\|_\infty < (\frac{1}{2} + \frac{1}{2} + C_rC_d)\frac{\epsilon}{1+C_rC_d} = \epsilon
\end{aligned}$$

□

C Proof of Lemma 2

Proof.

For sake of simplicity, for all $k \in \mathbb{Z}$ such that $k2^{-J} \in K$, we denote $L := L_{p,\epsilon}$, $L_\epsilon := L_{p,\frac{\epsilon/2}{1+C_rC_d}}$, $j_{f,k} := j_{p,\epsilon}((Lf)^J, k2^{-J})$, $j_{Lf,k} := j_{p,\frac{\epsilon/2}{1+C_rC_d}}((L_\epsilon f)^J, k2^{-J})$, $j_{g,k} := j_{p,\frac{\epsilon/2}{1+C_rC_d}}(g^J, k2^{-J})$, $j_{\Delta_n} := j_{\Delta_n,p,\epsilon}(f^J, k2^{-J})$ and $C(k) := C_{S_p}(k2^{-J})$.

We denote g^J the polygon constructed in Proposition 3 as the over-smoothing of $L_\epsilon X^J$. We recall that its local levels are at most the ones of $L_\epsilon f^J$, and that $\left\|X^J - g^J\right\|_\infty < \epsilon$. Then, g^J is a smoothing of X^J at distance ϵ from X, like LX^J.

As the smoothing algorithm processes the details ordered by decreasing level j, the local levels of LX^J are at most the ones of g^J, then at most the ones of $L_\epsilon f^J$ by construction of g^J.

Moreover, $L_\epsilon f^J$ is a $\frac{\epsilon/2}{1+C_rC_d}$−smoothing of f^J (with $\frac{\epsilon/2}{1+C_rC_d} < \epsilon$), then the local levels of Lf^J are also at most the ones of $L_\epsilon f^J$.

Finally, for all $i \in I_n$, $2^{-j_{f,k+i}} = O\left(\epsilon^{\frac{1}{p+1}}\right)$, so $2^{-j_{\Delta_n}} = O\left(\epsilon^{\frac{1}{p+1}}\right)$: then there exists $C_\epsilon > 0$ such that $2^{-j_{\Delta_n}} \leq C_\epsilon \epsilon^{\frac{1}{p+1}}$ for all $k \in \mathbb{Z}$ such that $k2^{-J} \in K$.

Using the stability of the multiresolution reconstruction related to the order n divided differences:

$$\begin{aligned}
\left|\left(\Delta_n\left(LX^J\right)\right)_k - \left(\Delta_n\left(Lf^J\right)\right)_k\right| &= \left|\Delta_n\left(LX^J - g^J + g^J - L_\epsilon f^J + L_\epsilon f^J - Lf^J\right)_k\right| \\
&\leq C_r \left[\sup_{(j_{\Delta_n},k_i)\in \bigcup_{i\in I_n} C(k+i)} \left|\left(\Delta_n\left(LX^{j_{\Delta_n}}\right)\right)_{k_i} - \left(\Delta_n g^{j_{\Delta_n}}\right)_{k_i}\right|\right. \\
&\quad + \sup_{(j_{\Delta_n},k_i)\in \bigcup_{i\in I_n} C(k+i)} \left|\left(\Delta_n g^{j_{\Delta_n}}\right)_{k_i} - \left(\Delta_n\left(L_\epsilon f^{j_{\Delta_n}}\right)\right)_{k_i}\right| \\
&\quad + \sup_{(j_{\Delta_n},k_i)\in \bigcup_{i\in I_n} C(k+i)} \left|\left(\Delta_n\left(L_\epsilon f^{j_{\Delta_n}}\right)\right)_{k_i} - \left(\Delta_n\left(Lf^{j_{\Delta_n}}\right)\right)_{k_i}\right| \\
&\quad + \sum_{j=j_{\Delta_n}+1}^{J} \left(\sup_{(j,k_i)\in \bigcup_{i\in I_n} C(k+i)} \left|d^{j-1}_{\Delta_n LX,k_i} - d^{j-1}_{\Delta_n g,k_i}\right|\right. \\
&\qquad + \sup_{(j,k_i)\in \bigcup_{i\in I_n} C(k+i)} \left|d^{j-1}_{\Delta_n g,k_i} - d^{j-1}_{\Delta_n L_\epsilon f,k_i}\right| \\
&\qquad \left.\left. + \sup_{(j,k_i)\in \bigcup_{i\in I_n} C(k+i)} \left|d^{j-1}_{\Delta_n L_\epsilon f,k_i} - d^{j-1}_{\Delta_n Lf,k_i}\right|\right)\right]
\end{aligned}$$

Relating the differences and details of the multiresolution decomposition of the divided differences to the counterparts for the polygon, we get:

$$\begin{aligned}
\left|\left(\Delta_n\left(Lf^J\right)\right)_k - \left(\Delta_n\left(LX^J\right)\right)_k\right| \leq C_r \sum_{i\in I_n} |c_{i,n}| &\left[2^{j_{\Delta_n} n} \sup_{(j_{\Delta_n},k_i)\in C(k+i)} \left|\left(LX^{j_{\Delta_n}}\right)_{k_i} - g^{j_{\Delta_n}}_{k_i}\right|\right. \\
&+2^{j_{\Delta_n} n} \sup_{(j_{\Delta_n},k_i)\in C(k+i)} \left|g^{j_{\Delta_n}}_{k_i} - \left(L_\epsilon f^{j_{\Delta_n}}\right)_{k_i}\right| \\
&+2^{j_{\Delta_n} n} \sup_{(j_{\Delta_n},k_i)\in C(k+i)} \left|\left(L_\epsilon f^{j_{\Delta_n}}\right)_{k_i} - \left(Lf^{j_{\Delta_n}}\right)_{k_i}\right| \\
+ \sum_{j=j_{\Delta_n}+1}^{J} 2^{jn} &\left(\sup_{(j,k_i)\in C(k+i)} \left|d^{j-1}_{LX,k_i} - d^{j-1}_{g,k_i}\right|\right. \\
&\quad + \sup_{(j,k_i)\in C(k+i)} \left|d^{j-1}_{g,k_i} - d^{j-1}_{L_\epsilon f,k_i}\right| \\
&\quad \left.\left. + \sup_{(j,k_i)\in C(k+i)} \left|d^{j-1}_{L_\epsilon f,k_i} - d^{j-1}_{Lf,k_i}\right|\right)\right]
\end{aligned}$$

Now, considering each term separately, we get for each of them, noted $\mathbb{RHS}_i, 1 \leq i \leq 6$:

-$\mathbb{RHS}_1$ LX^J and g^J are both at distance ϵ from X^J, then $\left\|LX^J - g^J\right\|_\infty < 2\epsilon$; moreover, using the stability of the multiresolution decomposition,

$$\sup_{(j_{\Delta_n},k_i)\in C(k+i)} \left|\left(LX^{j_{\Delta_n}}\right)_{k_i} - g^{j_{\Delta_n}}_{k_i}\right| \leq \left\|LX^{j_{\Delta_n}} - g^{j_{\Delta_n}}\right\|_\infty \leq C_d \left\|LX^J - g^J\right\|_\infty < 2C_d\epsilon \ ;$$

-$\mathbb{RHS}_2$ From the construction of g^J in Proposition 3,

$$\sup_{(j_{\Delta_n},k_i)\in C(k+i)} \left|g^{j_{\Delta_n}}_{k_i} - \left(L_\epsilon f^{j_{\Delta_n}}\right)_{k_i}\right| \leq \left\|g^{j_{\Delta_n}} - L_\epsilon f^{j_{\Delta_n}}\right\|_\infty < C_d \left\|L_\epsilon X^J - f^J\right\|_\infty < C_d \frac{\epsilon/2}{1+C_rC_d};$$

-$\mathbb{RHS}_3$ The local levels of $L_\epsilon f^J$ are higher than the ones of Lf^J, so these polygons equal each other at level j_{Δ_n}: then $\sup_{(j_{\Delta_n},k_i)\in C(k+i)} \left|\left(L_\epsilon f^{j_{\Delta_n}}\right)_{k_i} - \left(Lf^{j_{\Delta_n}}\right)_{k_i}\right| = 0$;

-$\mathbb{RHS}_4$ The local levels of LX^J are lower than those of g^J, so for all $i \in I_n$, the details of LX^J and g^J in the cone $C(k+i)$ are the same up to the local level of LX^J at position $(k+i)2^{-J}$; the sum can then be rewritten starting from this local level, if it is higher than j_{Δ_n}, and ending at $j_{Lf,k+i}$ the local level of g^J at position $(k+i)2^{-J}$;

-$\mathbb{RHS}_5$ For each $i \in I_n$, above level $j_{Lf,k+i}$, the details of both polygons are 0;

-$\mathbb{RHS}_6$ For each $i \in I_n$, both smoothings of f^J share the same details up to level $j_{f,k+i}$ included; above this level, using $j_{f,k+i} \leq j_{Lf,k+i}$ and the definition of local level, the details of Lf^J are 0, then only the details of $L_\epsilon f^J$ remain up to level $j_{Lf,k+i}$;

We get:

$$\begin{aligned}\left|\left(\Delta_n\left(Lf^J\right)\right)_k - \left(\Delta_n\left(LX^J\right)\right)_k\right| \leq C_r \sum_{i\in I_n} |c_{i,n}| \Bigg[& 2^{j_{\Delta_n} n}\left(2 + \frac{1/2}{1+C_rC_d}\right) C_d\epsilon \\ & + \sum_{j=\max\{j_{\Delta_n}, j_{LX,k+i}\}+1}^{j_{Lf,k+i}} 2^{jn} \sup_{(j,k_i)\in C(k+i)} \left|d^{j-1}_{g,k_i}\right| \\ & + \sum_{j=j_{\Delta_n}+1}^{j_{Lf,k+i}} 2^{jn} \sup_{(j,k_i)\in C(k+i)} \left|d^{j-1}_{g,k_i} - d^{j-1}_{L_\epsilon f,k_i}\right| \\ & + \sum_{j=j_{f,k+i}+1}^{j_{Lf,k+i}} 2^{jn} \sup_{(j,k_i)\in C(k+i)} \left|d^{j-1}_{L_\epsilon f,k_i}\right| \Bigg]\end{aligned}$$

Now, only the different sums on j have to be bounded with ϵ. For all $i \in I_n$:

1. For all $(j,k') \in C(k+i)$ such that $j \in \{j_{LX,k+i}+1, \ldots, j_{f,k+i}\}$, given that $\left\|g^J - LX^J\right\|_\infty < 2\epsilon$ and $d^{j-1}_{LX,k'} = 0$, then $\left\|d^{j-1}_g\right\|_\infty < 2C_d\epsilon$ using the stability of the multiresolution decomposition;
2. For all $(j,k') \in C(k+i)$ such that $j \in \{j_{\Delta_n}, \ldots, j_{f,k+i}\}$, using the stability of the multiresolution decomposition, the sum is bounded by $C_d \left\|g^J - L_\epsilon f^J\right\|_\infty$ given that $\left\|g^J - L_\epsilon f^J\right\|_\infty \leq \frac{C_rC_d\epsilon}{1+C_rC_d}$ from the construction of g^J;
3. For all $(j,k') \in C(k+i)$ such that $j \geq j_{Lf,k+i}$, using the decay of the details of f from Proposition 1, $\left\|d^{j-1}_{L_\epsilon f}\right\|_\infty < C_{dec}2^{-j(p+1)}$;

In the three cases, a sum over j remains.

Furthermore, we know that for all $j_1 < j_2$, $\sum_{j=j_1}^{j_2} 2^{jn} \leq 2^{(j_2+1)n}$, then all these sums over j are bounded by $2^{(j_{f,k+i}+1)n}$ for all $i \in I_n$.

Defining:

- $C' > 0$ such that for all $i \in I_n$, $\epsilon \leq C'2^{-(j_{f,k+i}+1)(p+1)}$ (then $\epsilon \leq C'2^{-(j_{\Delta_n}+1)(p+1)}$),
- $C_\epsilon > 0$ such that $2^{-(j_{\Delta_n}+1)} \leq C_\epsilon\epsilon^{\frac{1}{p+1}}$ for all $k \in \mathbb{Z}$ such that $k2^{-J} \in K$,

we then obtain, for all $k \in \mathbb{Z}$:

$$\begin{aligned}
\left|\left(\Delta_n\left(Lf^J\right)\right)_k - \left(\Delta_n\left(LX^J\right)\right)_k\right| &\leq C_r \sum_{i\in I_n} |c_{i,n}| C' \left[\left(2 + \frac{1/2}{1+C_rC_d}\right) C_d 2^{(j_{\Delta_n}+1)n} 2^{-(j_{\Delta_n}+1)(p+1)}\right. \\
&\qquad + 2C_d \times 2^{(j_{f,k+i}+1)n} 2^{-(j_{f,k+i}+1)(p+1)} \\
&\qquad \left. + \frac{C_rC_d}{1+C_rC_d} 2^{(j_{f,k+i}+1)n} 2^{-(j_{f,k+i}+1)(p+1)} + C_{dec} 2^{-(j_{f,k+i}+1)(p+1-n)}\right] \\
&\leq C_r \sum_{i\in I_n} |c_{i,n}| C' \left(\left(4 + \frac{1/2+C_r}{1+C_rC_d}\right) C_d + C_{dec}\right) 2^{-(j_{\Delta_n}+1)(p+1-n)} \\
&\leq C_r \sum_{i\in I_n} |c_{i,n}| C' \left(\left(4 + \frac{1/2+C_r}{1+C_rC_d}\right) C_d + C_{dec}\right) C_\epsilon \epsilon^{1-\frac{n}{p+1}}
\end{aligned}$$

$$\implies \left\|\Delta_n\left(Lf^J\right) - \Delta_n\left(LX^J\right)\right\|_{\infty,K} \leq C\epsilon^{1-\frac{n}{p+1}} \text{ defining } C := C_rC'C_\epsilon \left(\left(4 + \frac{1/2+C_r}{1+C_rC_d}\right) C_d + C_{dec}\right) \sum_{i\in I_n} |c_{i,n}|.$$

□

D Equations of the Lagrange schemes used in this paper

D.1 2-point interpolatory Lagrange, order $p = 1$, regularity $m = 0$

This scheme is the one used for the example illustration in Introduction. Among the Lagrange schemes introduced in this appendix, this scheme is the only one which does not require adaption at edges.

Subdivision :

$$\begin{cases} \left(SX^{j-1}\right)_{2k} = X_k^{j-1} \\ \left(SX^{j-1}\right)_{2k+1} = \frac{1}{2}\left(X_k^{j-1} + X_{k+1}^{j-1}\right) \end{cases} \tag{8}$$

Consistent decimation:

$$\left(DX^j\right)_k = X_{2k}^j \tag{9}$$

D.2 8-point shifted Lagrange, order $p = 8$, regularity $m = 4$

For this scheme, edge adaptations are given for the left boundary. The right boundary adaptations can be deduced by symmetry.

D.2.1 General equations

In Equations (10) and (11), coefficients were determined using Lagrange interpolation polynomials of degree 7 such that, for all $j \in \mathbb{Z}$ and all $k \in \mathbb{Z}$:

- $\left(SX^{j-1}\right)_{2k}$ is associated to position $\left(k - \frac{1}{4}\right) 2^{-(j-1)}$ between X_{k-1}^j and X_k^j,
- $\left(SX^{j-1}\right)_{2k+1}$ is associated to position $\left(k + \frac{1}{4}\right) 2^{-(j-1)}$ between X_k^j and X_{k+1}^j,
- $\left(DX^j\right)_k$ is associated to position $\left(2k + \frac{1}{2}\right) 2^{-j}$ between X_{2k}^j and X_{2k+1}^j.

Subdivision:

$$\begin{cases} \left(SX^{j-1}\right)_{2k} = \frac{1}{2^{18}}\Big(-429X_{k-4}^{j-1} + 4095X_{k-3}^{j-1} - 19305X_{k-2}^{j-1} + 75075X_{k-1}^{j-1} \\ \qquad\qquad +225225X_k^{j-1} - 27027X_{k+1}^{j-1} + 5005X_{k+2}^{j-1} - 495X_{k+3}^{j-1}\Big) \\ \left(SX^{j-1}\right)_{2k+1} = \frac{1}{2^{18}}\Big(-495X_{k-3}^{j-1} + 5005X_{k-2}^{j-1} - 27027X_{k-1}^{j-1} + 225225X_k^{j-1} \\ \qquad\qquad +75075X_{k+1}^{j-1} - 19305X_{k+2}^{j-1} + 4095X_{k+3}^{j-1} - 429X_{k+4}^{j-1}\Big) \end{cases} \tag{10}$$

Consistent decimation:

$$\begin{aligned} \left(DX^j\right)_k = \frac{1}{1000686485504}\Big(&1706176329X_{2k-7}^j - 1968664995X_{2k-6}^j - 12139784865X_{2k-5}^j \\ &+15121032355X_{2k-4}^j + 38694497985X_{2k-3}^j - 60840378027X_{2k-2}^j \\ &-87733282065X_{2k-1}^j + 607503646035X_{2k}^j + 607503646035X_{2k+1}^j \\ &-87733282065X_{2k+2}^j - 60840378027X_{2k+3}^j + 38694497985X_{2k+4}^j \\ &+15121032355X_{2k+5}^j - 12139784865X_{2k+6}^j - 1968664995X_{2k+7}^j \\ &+1706176329X_{2k+8}^j\Big) \end{aligned} \tag{11}$$

D.2.2 Edge adaptations

These new sets of coefficients are given when subdivision or decimation cannot be realized with an equal number of points at both sides of the predicted point, using the same original idea as in the previous Section D.2.1.

Subdivision:

$$\begin{cases}
\left(SX^{j-1}\right)_0 = \frac{1}{2^{18}}\left(480675X_0^{j-1} - 672945X_1^{j-1} + 1121575X_2^{j-1} - 1294125X_3^{j-1}\right. \\
\qquad\qquad \left. +989625X_4^{j-1} - 480675X_5^{j-1} + 134589X_6^{j-1} - 16575X_7^{j-1}\right) \\
\left(SX^{j-1}\right)_1 = \frac{1}{2^{18}}\left(129789X_0^{j-1} + 302841X_1^{j-1} - 389367X_2^{j-1} + 412965X_3^{j-1}\right. \\
\qquad\qquad \left. -302841X_4^{j-1} + 143451X_5^{j-1} - 39501X_6^{j-1} + 4807X_7^{j-1}\right) \\
\left(SX^{j-1}\right)_2 = \frac{1}{2^{18}}\left(16575X_0^{j-1} + 348075X_1^{j-1} - 208845X_2^{j-1} + 193375X_3^{j-1}\right. \\
\qquad\qquad \left. -133875X_4^{j-1} + 61425X_5^{j-1} - 16575X_6^{j-1} + 1989X_7^{j-1}\right) \\
\left(SX^{j-1}\right)_3 = \frac{1}{2^{18}}\left(-4807X_0^{j-1} + 168245X_1^{j-1} + 168245X_2^{j-1} - 120175X_3^{j-1}\right. \\
\qquad\qquad \left. +76475X_4^{j-1} - 33649X_5^{j-1} + 8855X_6^{j-1} - 1045X_7^{j-1}\right) \\
\left(SX^{j-1}\right)_4 = \frac{1}{2^{18}}\left(-1989X_0^{j-1} + 32487X_1^{j-1} + 292383X_2^{j-1} - 97461X_3^{j-1}\right. \\
\qquad\qquad \left. +54145X_4^{j-1} - 22491X_5^{j-1} + 5733X_6^{j-1} - 663X_7^{j-1}\right) \\
\left(SX^{j-1}\right)_5 = \frac{1}{2^{18}}\left(1045X_0^{j-1} - 13167X_1^{j-1} + 197505X_2^{j-1} + 109725X_3^{j-1}\right. \\
\qquad\qquad \left. -47025X_4^{j-1} + 17955X_5^{j-1} - 4389X_6^{j-1} + 495X_7^{j-1}\right) \\
\left(SX^{j-1}\right)_6 = \frac{1}{2^{18}}\left(663X_0^{j-1} - 7293X_1^{j-1} + 51051X_2^{j-1} + 255255X_3^{j-1}\right. \\
\qquad\qquad \left. -51051X_4^{j-1} + 17017X_5^{j-1} - 3927X_6^{j-1} + 429X_7^{j-1}\right)
\end{cases} \tag{12}$$

Consistent decimation:

$$\begin{cases}
\left(DX^j\right)_0 = \frac{1}{2^{11}}\left(429X_0^j + 3003X_1^j - 3003X_2^j + 3003X_3^j - 2145X_4^j + 1001X_5^j - 273X_6^j + 33X_7^j\right) \\
\left(DX^j\right)_1 = \frac{1}{2^{11}}\left(9X_0^j - 105X_1^j + 945X_2^j + 1575X_3^j - 525X_4^j + 189X_5^j - 45X_6^j + 5X_7^j\right) \\
\left(DX^j\right)_2 = \frac{1}{2^{11}}\left(5X_0^j - 45X_1^j + 189X_2^j - 525X_3^j + 1575X_4^j + 945X_5^j - 105X_6^j + 9X_7^j\right) \\
\left(DX^j\right)_3 = \frac{1}{2^{11}}\left(33X_0^j - 273X_1^j + 1001X_2^j - 2145X_3^j + 3003X_4^j - 3003X_5^j + 3003X_6^j + 429X_7^j\right)
\end{cases} \tag{13}$$